

Germany). The average size of the silica particles was determined to be 75.7, 311 and 830 nm by Zetasizer (Sysmex Co., Kobe, Japan). The particles were spherical and nonporous. The particles were stocked at 25 mg/ml (70 nm) and 50 mg/ml (300 and 1000 nm) in aqueous suspension. The stock solutions were suspended using vortex mixer for 5 min before use. The resultant solutions did not show aggregation of the particles by electron microscopy analysis. Reagents used in this study were of research grade.

2.2. Animals

BALB/c male mice (8 wk) were obtained from Shimizu Laboratory Supplies Co., Ltd. (Kyoto, Japan), and were housed in an environmentally controlled room at 23 ± 1.5 °C with a 12-h light/12-h dark cycle. Mice had free access to water and commercial chow (Type MF, Oriental Yeast, Tokyo, Japan). Mice were intravenously injected with the silica particles at 10–100 mg/kg body weight. The experimental protocols conformed to the ethical guidelines of the Graduate School of Pharmaceutical Sciences, Osaka University.

2.3. Histological analysis

The liver, kidney, spleen and lung were removed and fixed with 4% paraformaldehyde. After sectioning, thin tissue sections of tissues were stained with hematoxylin and eosin for histological observation. Liver sections were stained with Azan-Mallory for observation of liver fibrosis.

2.4. Biochemical assay

Serum alanine aminotransferase (ALT) levels and blood urea nitrogen (BUN) were measured using a commercially available Transaminase-CII kit and Blood Urea Nitrogen-B Test Wako (WAKO Pure Chemical, Osaka, Japan), respectively. Interleukin-6 (IL-6) and tumor necrosis factor- α (TNF- α) were measured with an ELISA kit (BioSource International, CA, USA).

2.5. Gadolinium chloride assay

For Kupffer cell blockage of phagocytosis and partial depletion in the liver, mice were injected intravenously with gadolinium chloride (GdCl_3) at 10 mg/kg body weight at 30 and 6 h prior to intravenous administration of nanoparticles [12,13]. Blood was then recovered 24 h after injection of nanoparticles for ALT assay.

2.6. Cyclophosphamide assay

Disruption of liver sinusoidal endothelial cells was carried out by intraperitoneal injection of 300 mg/kg body weight cyclophosphamide (CPA) at 24 h prior to administration of nanoparticles [14,15]. Blood was recovered at 24 h after injection of nanoparticles for ALT assay.

2.7. Hepatic hydroxyproline content

Hepatic hydroxyproline content was assayed by Kivirikko's method, with some modification [16]. Briefly, liver tissue was hydrolyzed in 6 M HCl at 110 °C for 24 h in a glass tube. After centrifugation, the resultant supernatant was neutralized with 8 N KOH, and 2 g of KCl and 1 ml of 0.5 M borate buffer were then added, followed by incubation for 15 min at room temperature and further incubation for 15 min at 0 °C. Chloramine-T solution was then prepared and added. After additional incubation for 1 h at 0 °C, 2 ml of 3.6 M sodium thiosulfate was added, followed by incubation at 120 °C for 30 min. Next, 3 ml of toluene was added

with incubation for a further 20 min at room temperature. After centrifugation, 2 ml of the resultant supernatant was added to Ehrlich's reagent, followed by incubation for 30 min at room temperature. Subsequently, the absorbance was measured at 560 nm.

2.8. Statistical analysis

Statistical analysis was performed by two-way ANOVA, followed by Student's *t*-test. The level of significance was set at $p < 0.05$.

3. Results

3.1. Liver injury by 70-nm silica nanoparticles

We initially investigated the acute toxicity of silica particles with diameters of 70 (SP70), 300 (SP300) or 1000 nm (SP1000) at maximal dose of 100 mg/kg. Intravenous injection of SP70 at 50 and 100 mg/kg was often lethal, but mice injected with SP300 and SP1000 survived. Fig. 1 shows hematoxylin–eosin staining of the liver, spleen, lung and kidney in silica particle-injected mice. We found no toxicity in any of these organs in SP300 or SP1000-injected mice at 100 mg/kg, and we found no abnormalities in the spleen, kidney and lung in SP70-injected mice at 30 mg/kg (Fig. 1A–D). However, degenerative necrosis of hepatocytes in the liver was observed in SP70-injected mice, thus suggesting that SP70 is toxic to the liver (Fig. 1A).

Next, in order to confirm the hepatotoxicity of SP70, we examined serum ALT activity, a biochemical marker of liver injury. Consistent with the histological data, injection of SP70 elevated serum ALT levels 35-fold over control values at 30 mg/kg, but injection of SP300 or SP1000 had no effect even at 100 mg/kg (Fig. 2A). Elevation of blood urea nitrogen, a biochemical marker of kidney injury, was not observed (Fig. 2B). Serum levels of inflammatory cytokine IL-6 and TNF- α were markedly elevated to 1124 and 80 pg/ml, respectively, in SP70-treated mice at 3 h (Fig. 2B and C). Slight elevation of serum IL-6 levels was observed in SP300- and SP1000-injected mice (28 and 32 pg/ml, respectively), while no elevation of TNF- α was observed. The IL-6 levels seen in SP300- or SP1000-treated mice were insufficient for liver injury. To investigate dose dependency of SP70-induced liver injury, we also investigated serum ALT and inflammatory cytokine levels at 12 h after SP70 administration. ALT, IL-6 and TNF- α levels were elevated in a dose-dependent manner after SP70 injection, and significant increases were observed with doses as low as 20 mg/kg (Fig. 3A–C). Taken together, these data suggest that 70-nm silica particles are toxic to the liver.

3.2. Involvement of Kupffer cells in SP70-induced liver injury

Kupffer cells are large liver macrophages, and are localized within the liver sinusoidal cells. Kupffer cells play a role in defense against various particles and substances entering the liver through the portal circulation [17]. Indeed, Kupffer cells clear virus particles from the bloodstream by phagocytosis [18–20]. The phagocytosis of parasites by Kupffer cells is accompanied by the release of pro-inflammatory cytokines that act as a paracrine signal to neighboring hepatocytes, and induce chemotaxis and aggregation of neutrophils. GdCl_3 inhibits phagocytosis by Kupffer cells and transiently eliminates Kupffer cells [12], and GdCl_3 has thus been widely used to investigate the roles of Kupffer cells in the liver [21,22]. To investigate the involvement of Kupffer cells in particle-induced liver injury, we evaluated the effects of GdCl_3 on nanoparticle-induced liver injury. As shown in Fig. 4A, pre-injection of GdCl_3 prior to injection of SP70 elevated serum ALT levels 5.5-fold

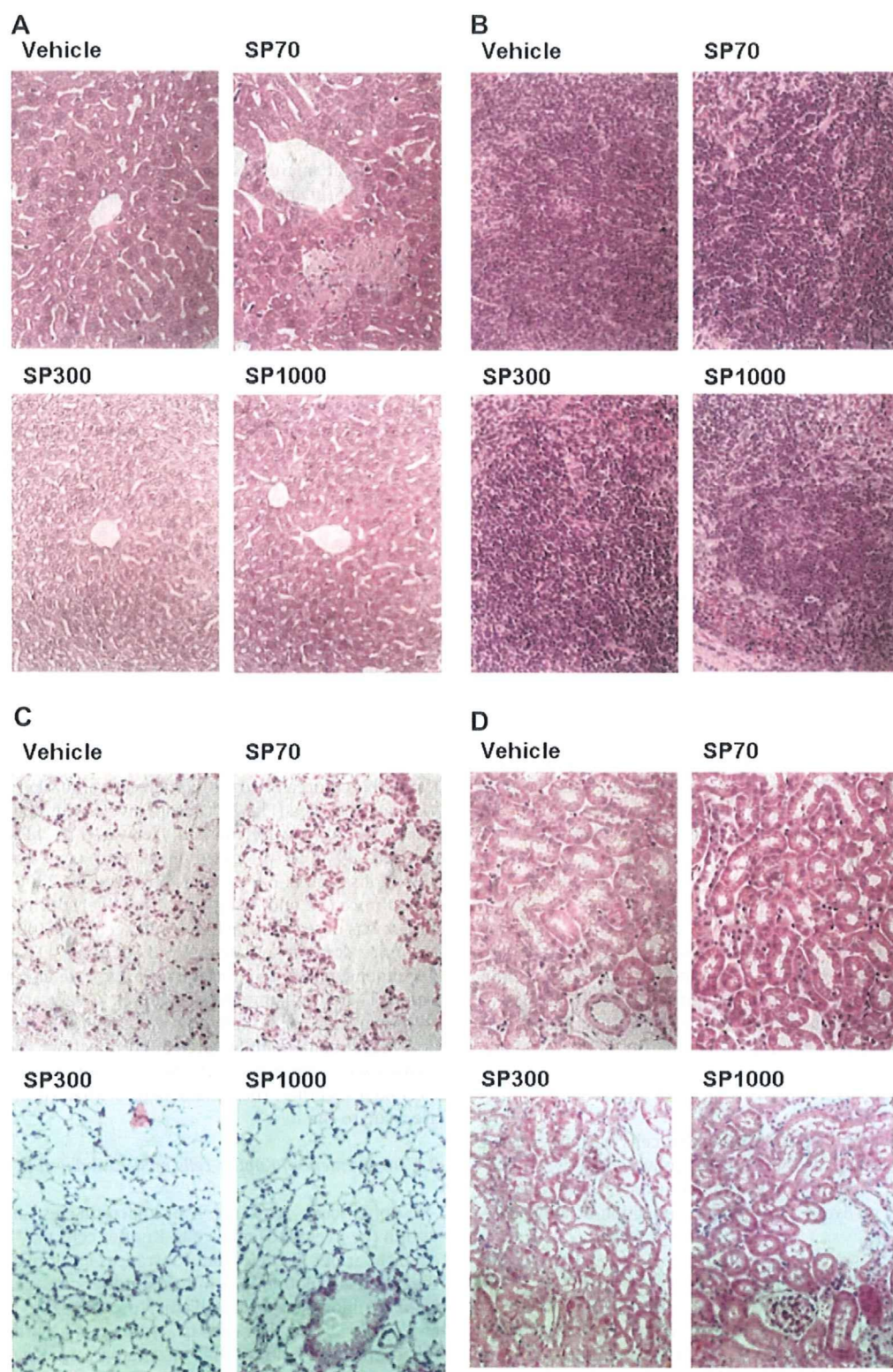


Fig. 1. Histological analysis of tissues in silica particle-treated mice. Silica particles with diameters of 70 (SP70), 300 (SP300) or 1000 nm (SP1000) were intravenously administered to mice at 30, 100 and 100 mg/kg, respectively. At 24 h after administration, tissues of liver (A), spleen (B), lung (C) and kidney (D) were collected, and fixed with 4% paraformaldehyde. Tissue sections were stained with hematoxylin and eosin and observed under a microscope. Data are representative of at least four mice.

in the SP70-injected group. In contrast, pre-injection of $GdCl_3$ did not affect ALT levels in the SP300- or SP1000-administered group. Taken together, these results indicate that phagocytosis of SP70 by

Kupffer cells may attenuate liver injury, but the release of proinflammatory cytokines from Kupffer cells is not associated with SP70-induced liver injury.

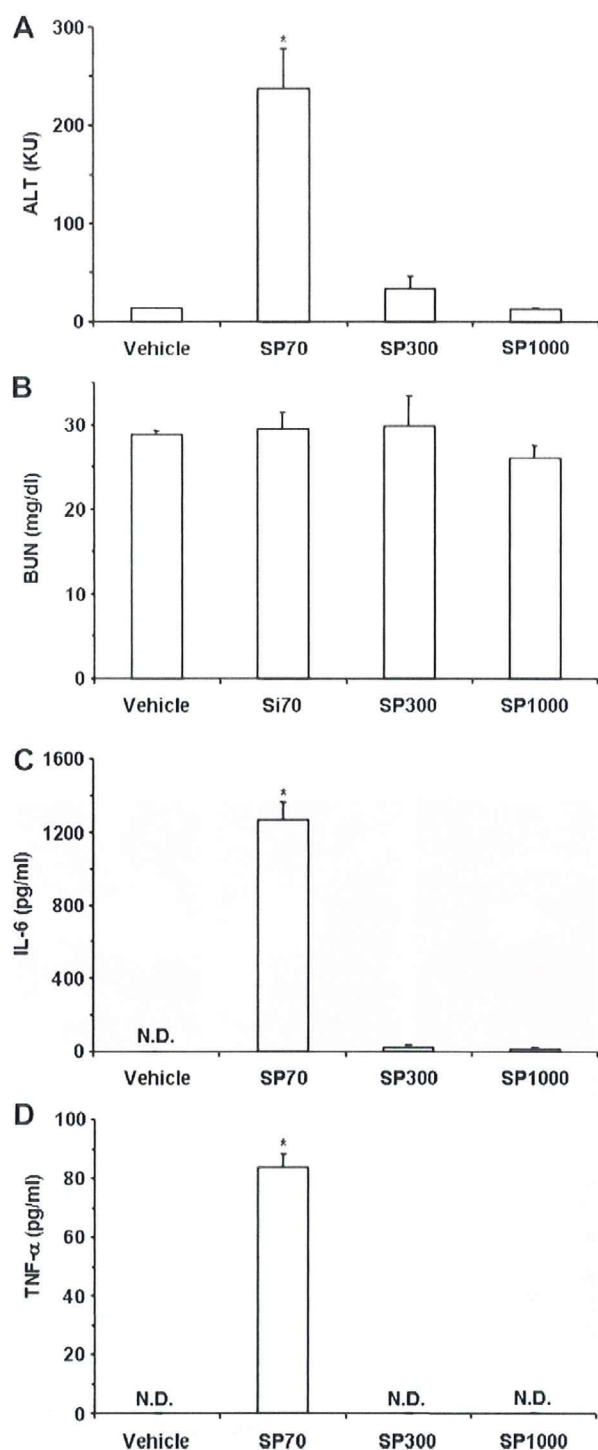


Fig. 2. Biochemical analyses of liver injury in silica particle-injected mice. SP70, SP300 or SP1000 was intravenously injected to mice at 30, 100 or 100 mg/kg, respectively. Blood was recovered at 3 and 24 h of the injection. Serum ALT (A) and BUN (B) at 24 h and IL-6 (C) and TNF-α (D) levels at 3 h were measured using a commercially available kit, as described in Section 2. Data are means \pm SEM ($n = 4$). *Significant difference vs. vehicle-treated group ($p < 0.05$).

3.3. Involvement of liver sinusoidal endothelial cells in SP70-induced liver injury

Sinusoidal endothelium forms a barrier between the blood-stream and hepatocytes, preventing passage of particles. Liver

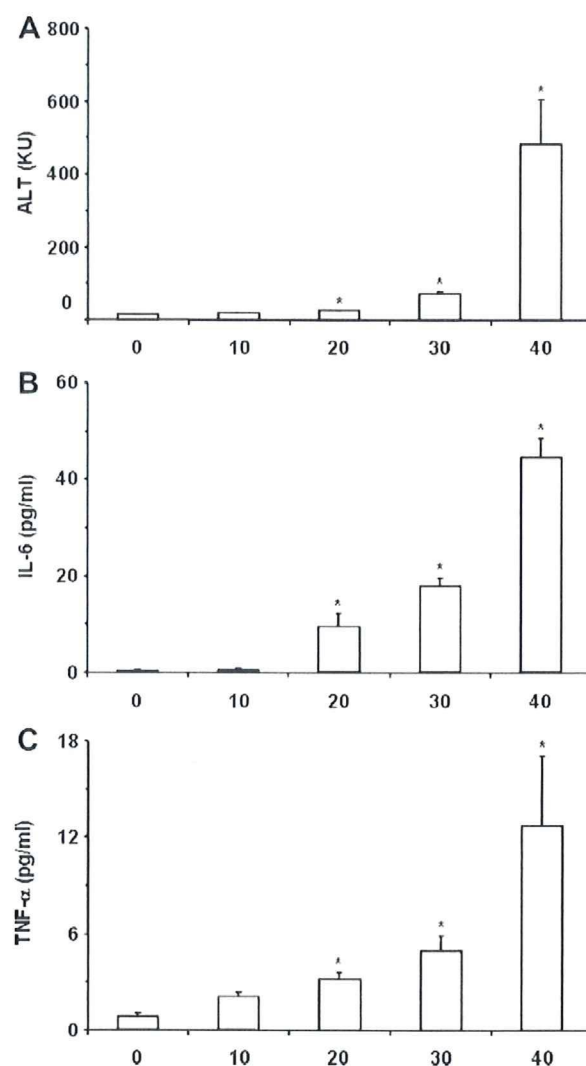


Fig. 3. Dose dependency of SP70 on liver injury. SP70 were intravenously administered at the indicated doses, and blood was recovered at 12 h after administration. Serum was used for measurement of ALT (A), IL-6 (B) and TNF-α (C), as described in Section 2. Data are means \pm SEM ($n = 4$). *Significant difference compared with the vehicle-treated group ($p < 0.05$).

sinusoidal endothelial cells (LSECs) are perforated by fenestrations, which are pores of approximately 100 nm in diameter. SP70, but not SP300 and SP1000, may pass through LSECs to the hepatocytes, resulting in liver injury. To evaluate this hypothesis, we performed CPA assay. CPA is converted in the liver to toxic metabolites, 4-hydroperoxycyclophosphamide and acrolein, to which endothelial cells are 20-fold more susceptible than hepatocytes [14]. CPA has been shown to disrupt LSECs [14,15]. We thus investigated the effects of CPA on nanoparticle-induced liver injury. As shown in Fig. 4B, pre-injection of CPA did not affect ALT levels in SP300- or SP1000-administered mice, whereas CPA dramatically decreased ALT levels to near control values in SP70-injected mice (from 235 to 29 KU). These data on CPA indicate that LSECs may be directly or indirectly involved in SP70-induced liver injury, but may not be a barrier against SP70.

3.4. Chronic toxicity of SP70

Finally, we investigated the effects of SP70 on chronic liver injury. SP70 was injected into mice every 3 days for 4 weeks at 10 or 30 mg/kg. The lower dose (10 mg/kg) did not cause acute liver

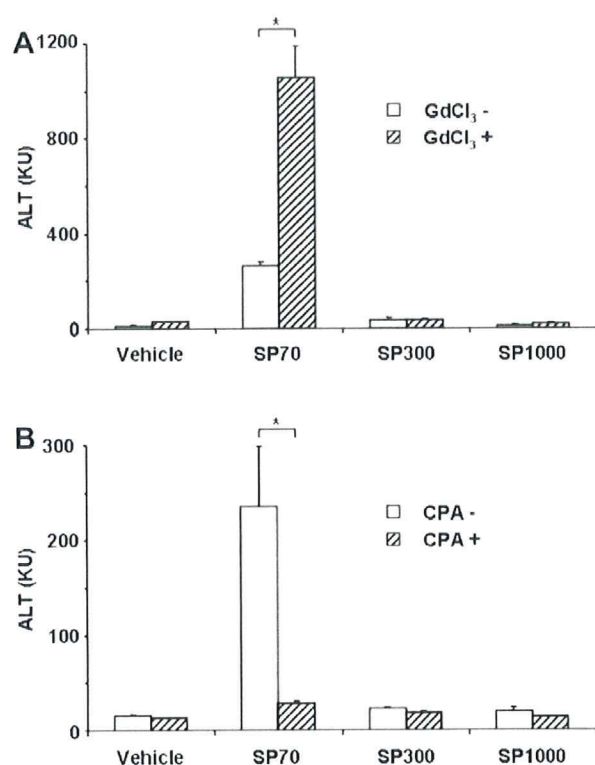


Fig. 4. Pharmaceutical analysis of SP70-induced liver injury. (A) GdCl₃ assay. Vehicle or GdCl₃ (10 mg/kg) was intravenously injected into mice at 30 h or 6 h prior to treatment with silica particles (SP70, 30 mg/kg; SP300, 100 mg/kg; SP1000, 100 mg/kg). At 24 h after particle administration, blood was recovered, and the resultant serum was used for ALT assay. Data are means \pm SEM ($n = 4$). *Significant difference between vehicle- and silica particle-treated groups ($p < 0.05$). (B) CPA assay. Vehicle or CPA (300 mg/kg) was intraperitoneally injected to mice at 24 h prior to treatment with silica particles. At 24 h after administration of particles, blood was recovered, and the resultant serum was used for ALT assay. Data are means \pm SEM ($n = 4$). *Significant difference between vehicle- and silica particle-treated groups ($p < 0.05$).

failure (Fig. 3A). Histological analysis demonstrated that chronic exposure of SP70-induced denaturation of hepatocytes in a dose-dependent manner (Fig. 5A). Serum ALT levels were also elevated by SP70 administration (Vehicle, 14.3 KU; SP70, 24.8 and 42.1 KU at 10 and 30 mg/kg, respectively) (Fig. 5B). Liver fibrosis is a symptom of chronic liver injury, and thus, we investigated liver fibrosis. Collagen, which is accumulated in the fibrotic liver, was stained with Azan reagent, and blue-stained regions were observed in SP70-treated, but not vehicle-treated, liver sections (Fig. 5C). Elevated hydroxyproline content parallels the extent of fibrosis, and we investigated the hydroxyproline contents in the SP70-treated mouse liver. Injection of SP70 significantly elevated hepatic hydroxyproline contents 1.6- and 3.5-fold over control values, at 10 mg/kg and 30 mg/kg, respectively (Fig. 5D). These data indicate that chronic administration of SP70 causes liver fibrosis, even at doses that are non-toxic in a single injection.

4. Discussion

In the present study, we evaluated the acute toxicity of silica particles with a diameter of 70, 300 or 1000 nm, and we found that 70-nm silica particles injure the liver, but not the spleen, lung or kidney. Moreover, chronic administration of 70-nm silica particles caused liver fibrosis, even at doses that were non-toxic in a single injection.

Surface area is a critical factor for toxicity of nano-size particles in the liver. The numbers of particles of SP70, 300 and 1000 are 2.8×10^{12} , 3.5×10^{10} and 9.5×10^8 particles/mg, respectively.

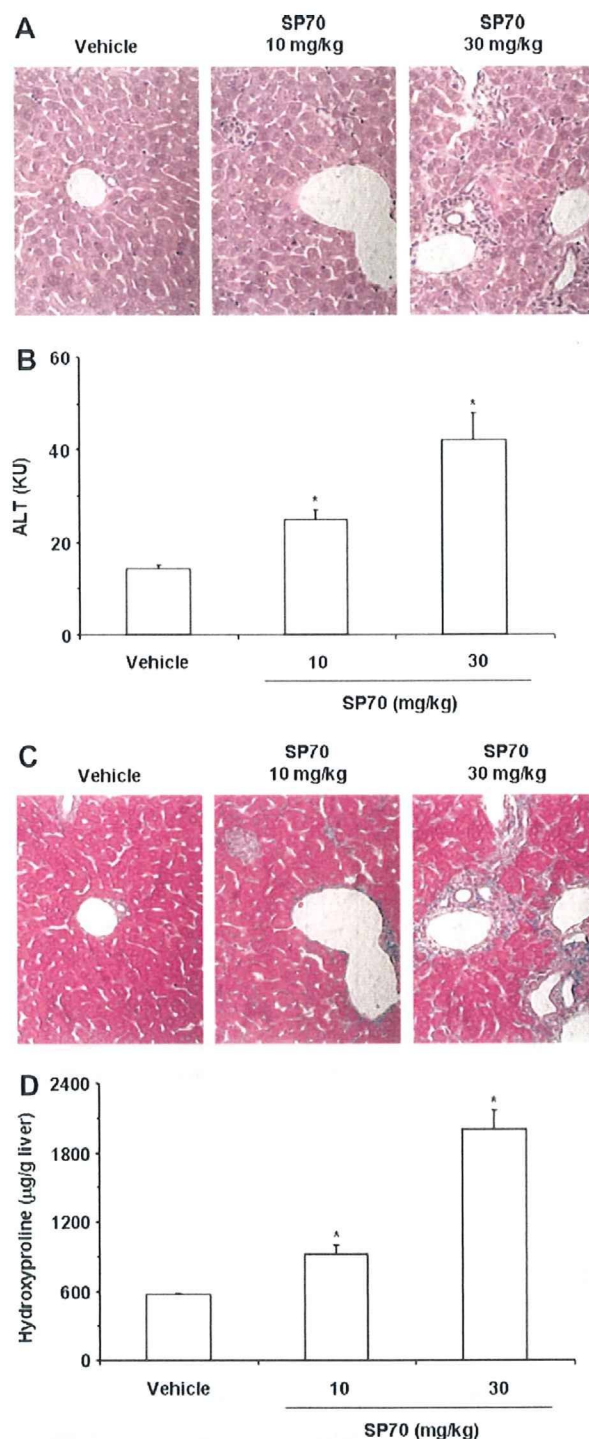


Fig. 5. Effect of SP70 on chronic liver injury. Mice were subjected to repeated administration of SP70 (10 or 30 mg/kg) every 3 days for 4 weeks. At 3 days after the last administration, mice were sacrificed. Tissues of livers were fixed with 4% paraformaldehyde, and liver sections were then stained with hematoxylin and eosin (A) or Azan (C). Hydroxyproline levels in the liver were assayed as described in Section 2 (C). Serum samples were used for measurement of ALT (B). (A and C) Data are representative of at least eight mice. (B) Data are means \pm SEM ($n = 4$). *Significant difference vs. vehicle-treated group ($p < 0.05$).

The surface area of SP300 at 100 mg/kg, at which SP300 was not toxic, is similar to that of SP70 at 30 mg/kg, at which SP70 was toxic. Difference in the surface area may not affect the different toxicities in the liver between SP70 and 300.

There are highly specialized endothelial cells, LSECs, in the liver, and these separate sinusoidal blood from hepatocytes. Passage of particles through LSECs is the first step for translocation from the bloodstream to hepatocytes. LSECs have fenestrations with a diameter of 100 nm, and the liver injury seen with 70-nm silica particles may be due to the particle size. We investigated the role of LSECs in the particle-induced liver injury using CPA, a disruptor of LSECs [13–15]. Unexpectedly, the disruption of LSEC did not cause SP300- and SP1000-induced liver injury. These results were consistent with the previous report that disruption of LSECs by CPA did not affect the hepatocyte transduction of a lentivirus vector with a diameter of 120–200 nm larger than the fenestrations of LSECs [13]. In contrast, SP70-induced liver injury was dramatically suppressed by disruption of LSECs, and pores in the LSEC may be responsible for the hepatic toxicity of SP70. Spaces, called the space of Disse, exist between LSEC and hepatocytes [23]. Particles entering into these spaces can avoid efflux into the blood flow in the sinusoids of the liver, resulting that this may enhance interaction between the particles and hepatocytes. Thus, the Disse spaces between LSECs and hepatocytes may be responsible for the liver injury caused by SP70.

Resident macrophages in the liver, Kupffer cells play a pivotal role in defense against foreign particles by eliminating such particles via phagocytosis [17]. $GdCl_3$ has been widely used to block phagocytosis by Kupffer cells and to deplete Kupffer cells [12,13,20,21]. Inactivation of Kupffer cells had no effect on SP300 and SP1000 treatment, whereas pre-treatment with $GdCl_3$ led to increased liver injury by SP70. There is no evidence that $GdCl_3$ exerts any direct toxic effects on hepatocytes, LSECs, or on other cells in the liver [24]. Thus, the elevation of SP70 toxicity may be caused by the depletion of Kupffer cells. Depletion of Kupffer cells enhanced the transgene activity of adenovirus vectors with a similar size with SP70 in the liver [22]. Therefore, inhibition of phagocytosis of Kupffer cells may enhance the interaction between SP70 and hepatocytes by increase in SP70 moving into the Disse spaces. Inhalation of silica particles causes lung injury [25], and alveolar macrophages function as a defense against inhaled agents, including viruses and environmental particles, via phagocytosis [26]. Macrophage receptor with collagenous structure (MARCO), CD204 and CD36 are reported to be the receptors for inert particles [26–30]. Uptake of silica particles through MARCO or CD204 induces cytotoxicity in alveolar macrophages, leading to lung fibrosis [30,31]. Alveolar macrophages from BALB/c do not express MARCO and CD204, and silica particles are taken up through CD36 [30]. Thus, uptake of SP70 by Kupffer cells through CD36 might not trigger liver injury. In this study, we found that chronic administration of SP70 caused liver fibrosis, even at 10 mg/kg body weight, at which level acute liver injury was not observed after a single injection. Nano-size particles-induced continuous inflammation in the liver will cause liver fibrosis leading to hepatic cancer.

Further evaluation of relationship between toxicity and variety of sizes, shapes, and chemical modification on the surface of particles is needed, and the future studies based on these data will provide very useful information on future development of drug delivery system using nano-size materials.

Acknowledgements

The authors thank all members of our laboratory for their useful comments and discussion. This study was supported by a grant from the Ministry of Health, Labor, and Welfare of Japan.

References

- [1] R.F. Service, U.S. nanotechnology. Health and safety research slated for sizable gains, *Science* 315 (2007) 926.
- [2] A. Nel, T. Xia, L. Madler, N. Li, Toxic potential of materials at the nanolevel, *Science* 311 (2006) 622–627.
- [3] G. Oberdorster, E. Oberdorster, J. Oberdorster, Nanotoxicology: an emerging discipline evolving from studies of ultrafine particles, *Environ. Health Perspect.* 113 (2005) 823–839.
- [4] J.S. Kim, T.J. Yoon, K.N. Yu, B.G. Kim, S.J. Park, H.W. Kim, K.H. Lee, S.B. Park, J.K. Lee, M.H. Cho, Toxicity and tissue distribution of magnetic nanoparticles in mice, *Toxicol. Sci.* 89 (2006) 338–347.
- [5] S. Takenaka, E. Karg, C. Roth, H. Schulz, A. Ziesenis, U. Heinzmann, P. Schramel, J. Heyder, Pulmonary and systemic distribution of inhaled ultrafine silver particles in rats, *Environ. Health Perspect.* 109 (Suppl. 4) (2001) 547–551.
- [6] A. Nemmar, P.H. Hoet, B. Vanquickenborne, D. Dinsdale, M. Thomeer, M.F. Hoylaerts, H. Vanbilloen, L. Mortelmans, B. Nemery, Passage of inhaled particles into the blood circulation in humans, *Circulation* 105 (2002) 411–414.
- [7] A. Nemmar, H. Vanbilloen, M.F. Hoylaerts, P.H. Hoet, A. Verbruggen, B. Nemery, Passage of intratracheally instilled ultrafine particles from the lung into the systemic circulation in hamster, *Am. J. Respir. Crit. Care Med.* 164 (2001) 1665–1668.
- [8] M. Vallet-Regi, F. Balas, D. Arcos, Mesoporous materials for drug delivery, *Angew. Chem. Int. Ed. Engl.* 46 (2007) 7548–7558.
- [9] S.D. Caruthers, S.A. Wickline, G.M. Lanza, Nanotechnological applications in medicine, *Curr. Opin. Biotechnol.* 18 (2007) 26–30.
- [10] Z. Medarova, W. Pham, C. Farrar, V. Petkova, A. Moore, In vivo imaging of siRNA delivery and silencing in tumors, *Nat. Med.* 13 (2007) 372–377.
- [11] M. Bottini, F. D'Annibale, A. Magrini, F. Cerignoli, Y. Arimura, M.I. Dawson, E. Bergamaschi, N. Rosato, A. Bergamaschi, T. Mustelin, Quantum dot-doped silica nanoparticles as probes for targeting of T-lymphocytes, *Int. J. Nanomed.* 2 (2007) 227–233.
- [12] M.J. Hardonk, F.W. Dijkhuis, C.E. Hulstaert, J. Koudstaal, Heterogeneity of rat liver and spleen macrophages in gadolinium chloride-induced elimination and repopulation, *J. Leukoc. Biol.* 52 (1992) 296–302.
- [13] N.P. van Til, D.M. Markusic, R. van der Rijt, C. Kunne, J.K. Hiralall, H. Vreeling, W.M. Frederiks, R.P. Oude-Elferink, J. Seppen, Kupffer cells and not liver sinusoidal endothelial cells prevent lentiviral transduction of hepatocytes, *Mol. Ther.* 11 (2005) 26–34.
- [14] L.D. DeLeve, Cellular target of cyclophosphamide toxicity in the murine liver: role of glutathione and site of metabolic activation, *Hepatology* 24 (1996) 830–837.
- [15] H. Malhi, P. Annamalai, S. Slehra, B. Joseph, K.K. Bhargava, C.J. Palestro, P.M. Novikoff, S. Gupta, Cyclophosphamide disrupts hepatic sinusoidal endothelium and improves transplanted cell engraftment in rat liver, *Hepatology* 36 (2002) 112–121.
- [16] K.I. Kivirikko, O. Laitinen, D.J. Prockop, Modifications of a specific assay for hydroxyproline in urine, *Anal. Biochem.* 19 (1967) 249–255.
- [17] K. Decker, Biologically active products of stimulated liver macrophages (Kupffer cells), *Eur. J. Biochem.* 192 (1990) 245–261.
- [18] K.T. Brunner, D. Hurez, C.R. Mc, B. Benacerraf, Blood clearance of P32-labeled vesicular stomatitis and Newcastle disease viruses by the reticuloendothelial system in mice, *J. Immunol.* 85 (1960) 99–105.
- [19] L. Zhang, P.J. Dailey, A. Gettie, J. Blanchard, D.D. Ho, The liver is a major organ for clearing simian immunodeficiency virus in rhesus monkeys, *J. Virol.* 76 (2002) 5271–5273.
- [20] R. Alemany, K. Suzuki, D.T. Curiel, Blood clearance rates of adenovirus type 5 in mice, *J. Gen. Virol.* 81 (2000) 2605–2609.
- [21] A. Lieber, C.Y. He, L. Meuse, D. Schowalter, I. Kirillova, B. Winther, M.A. Kay, The role of Kupffer cell activation and viral gene expression in early liver toxicity after infusion of recombinant adenovirus vectors, *J. Virol.* 71 (1997) 8798–8807.
- [22] G. Schiedner, S. Hertel, M. Johnston, V. Dries, N. van Rooijen, S. Kochanek, Selective depletion or blockade of Kupffer cells leads to enhanced and prolonged hepatic transgene expression using high-capacity adenoviral vectors, *Mol. Ther.* 7 (2003) 35–43.
- [23] E. Wisse, R.B. De Zanger, K. Charels, P. Van Der Smitten, R.S. McCuskey, The liver sieve: considerations concerning the structure and function of endothelial fenestrae, the sinusoidal wall and the space of Disse, *Hepatology* 5 (1985) 683–692.
- [24] R.M. Rai, S.Q. Yang, C. McClain, C.L. Karp, A.S. Klein, A.M. Diehl, Kupffer cell depletion by gadolinium chloride enhances liver regeneration after partial hepatectomy in rats, *Am. J. Physiol.* 270 (1996) G909–G918.
- [25] G.S. Cooper, F.W. Miller, D.R. Germolec, Occupational exposures and autoimmune diseases, *Int. Immunopharmacol.* 2 (2002) 303–313.
- [26] M. Arredouani, Z. Yang, Y. Ning, G. Qin, R. Soininen, K. Tryggvason, L. Kobzik, The scavenger receptor MARCO is required for lung defense against pneumococcal pneumonia and inhaled particles, *J. Exp. Med.* 200 (2004) 267–272.
- [27] L. Kobzik, Lung macrophage uptake of unopsonized environmental particulates. Role of scavenger-type receptors, *J. Immunol.* 155 (1995) 367–376.
- [28] M.S. Arredouani, A. Palecanda, H. Koziel, Y.C. Huang, A. Imrich, T.H. Sulhian, Y.Y. Ning, Z. Yang, T. Pikkarainen, M. Sankala, S.O. Vargas, M. Takeya, K. Tryggvason, L. Kobzik, MARCO is the major binding receptor for unopsonized particles and bacteria on human alveolar macrophages, *J. Immunol.* 175 (2005) 6058–6064.
- [29] A. Palecanda, J. Paulauskis, E. Al-Mutairi, A. Imrich, G. Qin, H. Suzuki, T. Kodama, K. Tryggvason, H. Koziel, L. Kobzik, Role of the scavenger receptor MARCO in alveolar macrophage binding of unopsonized environmental particles, *J. Exp. Med.* 189 (1999) 1497–1506.
- [30] R.F. Hamilton Jr., S.A. Thakur, J.K. Mayfair, A. Holian, MARCO mediates silica uptake and toxicity in alveolar macrophages from C57BL/6 mice, *J. Biol. Chem.* 281 (2006) 34218–34226.
- [31] R.F. Hamilton Jr., S.A. Thakur, A. Holian, Silica binding and toxicity in alveolarmacrophages, *Free Radic. Biol. Med.* 44 (2008) 1246–1258.

Laboratory of Bio-Functional Molecular Chemistry¹, Laboratory of Toxicology², Graduate School of Pharmaceutical Sciences, Osaka University; Laboratory of Pharmaceutical Proteomics³, Division of Biomedical Research, National Institute of Biomedical Innovation, Ibaraki, Osaka, Japan

Influence of 70 nm silica particles in mice with cisplatin or paraquat-induced toxicity

H. NISHIMORI¹, M. KONDOH¹, K. ISODA¹, S. TSUNODA³, Y. TSUTSUMI^{2,3}, K. YAGI¹

Received February 10, 2009, accepted February 21, 2009

Masuo Kondoh, Ph.D., Laboratory of Bio-Functional Molecular Chemistry,
Graduate School of Pharmaceutical Sciences, Osaka University, Suita, Osaka 565-0871, Japan
masuo@phs.osaka-u.ac.jp

Pharmazie 64: 395–397 (2009)

doi: 10.1691/ph.2009.9048

In the pharmaceutical industry, nano-size materials are designed as drug carriers and diagnosis probes. Interactions between nano-size materials and chemicals need investigating. Here, we investigated whether nano-size materials affect chemical-induced toxicity using silica particles, which have been widely used in cosmetics and drug delivery and have diameters of 70 (SP70), 300 (SP300) and 1000 (SP1000) nm, a popular anti-tumor agent, cisplatin, and a widely used herbicide, paraquat. Mice were treated with either cisplatin (100 μ mol/kg, intraperitoneally) or paraquat (50 mg/kg, intraperitoneally), with or without intravenous silica particle administration. All treatments were non-lethal and did not show severe toxicity, except for injection with both cisplatin and SP70, which were lethal. When mice received with paraquat and/or the silica particles, synergistic enhanced toxicity was observed in both paraquat- and SP70-treated mice. These synergic effects were not observed with either Si300 or 1000 treatment. Our findings suggest that further evaluation on the interaction between nano-size materials and chemicals is critical for the pharmaceutical application of nanotechnology.

1. Introduction

Nano-size materials are typically defined as engineered structures having at least one dimension of 100 nm or less. Changing from micro- to nano-size in materials expands surface area. In addition, nano-sized materials may have unique physicochemical properties due to their small size, chemical composition, surface structure, solubility, and shape. Recent development of nano-size particles from the micro- to nano-scale provides us with new tools, not only for industrial use such as electronics and catalysts, but also for pharmaceutical use such as cosmetics, diagnostic imaging and drug delivery (Caruthers et al. 2007; Vallet-Regi et al. 2007; Bartlett et al. 2007; Medarova et al. 2007). Although an expanded surface area of nano-size materials is advantageous, wide surface area can be accompanied by increasing interactions with biological tissues, cells, proteins, and nucleic acids, leading to toxic effects on humans (Nel et al. 2006; Oberdorster et al. 2005; Fischer and Chan, 2007). It is rare for a human to be exposed to only nano-size materials; we are often exposed to nano-size materials as well as other substances, such as xenobiotics and pharmaceutical agents. Nano-silica particles are intended for cosmetics and systemic and local delivery of drugs (Vallet-Regi et al. 2007). Previously, we found that intravenous administration of 70 nm, but not 300- and 1000 nm, silica particles caused liver injury (Nishimori et al. in press). Taken together, the synergistic effect of nano-size materials with other toxic substances should be evaluated, as there are few studies to date.

In this study, we investigated the synergistic effect of 70 nm silica particles with chemicals using cisplatin, a widely used anti-tumor agent (Ozols and Young 1991; Hartmann et al. 1999; Witjes 1997), and paraquat, one of the most widely used and highly toxic herbicides (Vandenbogaerde et al. 1984), providing evidence for synergistically enhanced toxicity.

2. Investigations and results

We previously found that intravenous administration of 70 nm size silica particles (SP70) caused liver failure, but 300- (SP300) and 1000- (SP1000) nm size particles did not (Nishimori et al. in press). Here, we investigated whether interaction between chemicals and silica particles occurred. To avoid direct interactions between chemicals and silica-particles before administration and absorption, we injected chemicals and silica-particles intraperitoneally and intravenously, respectively. Administration of cisplatin has been shown to cause adverse effects such as hepatic and renal failure (Lu and Cederbaum 2006; Ramesh et al. 2007). Indeed, serum levels of biochemical markers for hepatic and renal injury were elevated by cisplatin as shown in Fig. 1A and B, respectively. Co-treatment with cisplatin and SP300/1000 did not exhibit severe toxicity, whereas co-administration with cisplatin and SP70 showed lethal toxicity. Although SP70 did not show hepatic toxicity at 20 mg/kg, co-administration of SP70 with cisplatin caused the death of 5 of the 8 mice (Fig. 1). The surviving

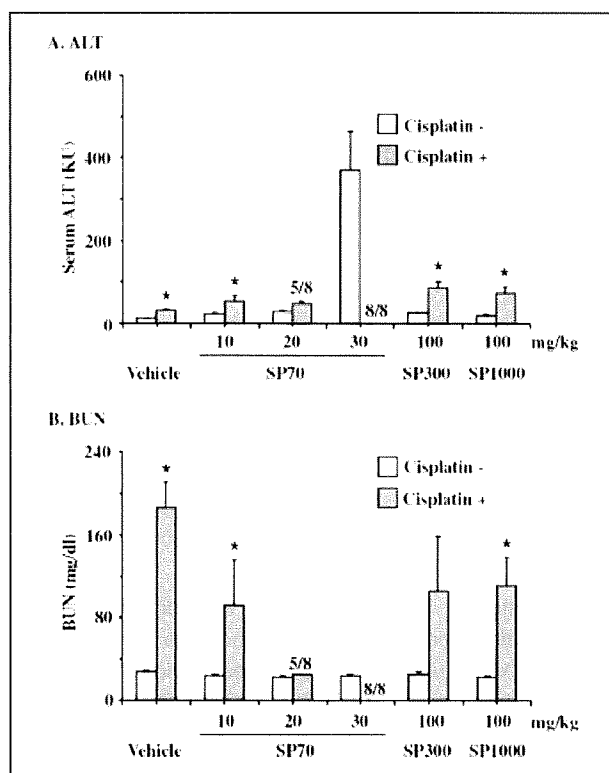


Fig. 1: Effect of SP70 on cisplatin-induced toxicity

Mice were injected with cisplatin at 0 (open column) or 100 μ mol/kg (filled column) and each silica particle (SP70, 70 nm particles; SP300, 300 nm particles; SP1000, 1000 nm particles) at the indicated dose, intraperitoneally and intravenously, respectively. At 24 h post-injection, the serum was recovered. ALT (A) and BUN (B) levels were assayed as described in the Materials and methods. Five of 8 and 8 of 8 mice died in the 20 mg/kg SP70/cisplatin and 30 mg/kg SP70/cisplatin-injected group, respectively. Data are representative of three independent experiments. Data are mean \pm SEM (n = 4–12). *Significant difference between vehicle and cisplatin-treated group (p < 0.05)

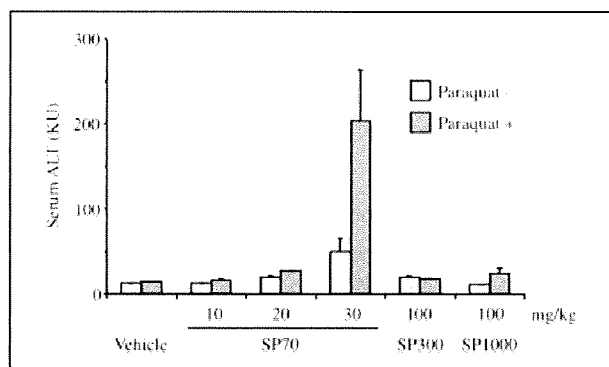


Fig. 2: Effect of SP70 on paraquat-induced toxicity

Mice were injected with paraquat at 0 (open column) or 50 mg/kg (filled column) and silica particles (SP70, SP300 or SP1000) at the indicated dose, intraperitoneally and intravenously, respectively. At 24 h post-injection, the serum was recovered. ALT levels were assayed as described in the Materials and methods. Data are representative of two independent experiments. Data are the mean \pm SEM (n = 4)

mice did not show abnormal ALT and BUN levels. SP70 did not show a lethal effect on mice at 30 mg/kg, but all mice injected with SP70 (30 mg/kg) died. We next investigated the interaction between paraquat and silica particles. Co-administration of paraquat (50 mg/kg) and silica par-

ticles did not elevate serum ALT, and SP70 showed synergistic elevation of serum ALT levels from 48.9 to 203.4 KU (Fig. 2). Synergistic effects of paraquat on SP300 or 1000 were not observed.

3. Discussion

In this study, we investigated the combined effects of chemicals on nano-size particle-induced toxicity, and found cisplatin and paraquat had synergistic toxic effects with silica particles with a diameter of 70 nm.

One characteristic of nano-size materials is their large surface area, and one explanation for the differing synergistic effects of nano- and macro-size particles is this difference in surface area. Indeed surface areas of SP300 and 1000 are 0.229 and 0.0068 per gram of particles relative to that of SP70, respectively. Lethality and ALT levels in cisplatin and paraquat, respectively, were observed with the injection of SP70 at 20 mg/kg, but not SP300 at 100 mg/kg, at which point the surface area of SP300 is almost equal to that of SP70. Therefore, the influence surface area has on the additive toxicity may be negligible. We previously found that differing hepatotoxicity among SP70, 300 and 1000 might be due to the accumulation of SP70 in the Disse space between liver sinusoidal endothelial cells and hepatocytes (Nishimori et al. in press). Differences in silica particle dynamics may be responsible for the synergistic effects of SP70. The profile of absorbed proteins on silica particles differed with particle size, and the amount of absorbed proteins was dependent on surface area; i.e., smaller particles absorbed more proteins on the surface (Dutta et al. 2007). The most abundant serum protein is albumin, and chemicals absorbed into the systemic circulation are often absorbed onto albumin. The structurally altered albumin is rapidly cleared from the circulation by a scavenger receptor (Demoy et al. 1999; Jansen et al. 1991; Kamps et al. 1997). The albumin-chemical complexes may be absorbed onto SP70, resulting in the aggregation of chemicals onto SP70 particles through albumin. Lipid-coated aggregation of cisplatin increased the cytotoxicity to 1000-fold compared with free drugs (Burger et al. 2002). The aggregated particles containing high dose of chemicals might be taken up, leading to enhanced toxicity. We will perform further biochemical and comprehensive analyses, such as proteome and genome assays, to determine the mechanism of these synergistic effects.

This report indicates synergistic toxicity of a nano-size silica particle with chemical agents. Further evaluation of such interactions between nano-size materials and pharmaceutical agents for future pharmaceutical application of nanotechnology are necessary.

4. Experimental

4.1. Materials

Silica particles with a diameter of 70, 300, or 1000 nm were obtained from Micromod Partikeltechnologie GmH (Rostock, Germany). The size distribution of the particles was analyzed by a Zetasizer (Sysmex Co., Kobe, Japan), and mean diameters were 55.7, 296, and 989 nm, respectively. The particles were spherical and nonporous, and stored at 25 mg/ml (70 nm) and 50 mg/ml (300 and 1000 nm) in aqueous suspension. The suspensions were thoroughly dispersed with sonication before use and diluted in water. An equal volume of solution was injected in each treatment. Paraquat and cisplatin were dissolved in saline and stored at -20°C before use. All reagents used were of research grade.

4.2. Animals

The 8-week-old BALB/c male mice were purchased from Shimizu Laboratory Supplies Co., Ltd. (Kyoto, Japan). They were maintained in controlled

environment (temperature: $23 \pm 1.5^\circ\text{C}$; light: 12 h light/dark cycle) with free access to standard rodent chow and water. The mice were given 1 week to adapt before commencing. The experimental protocols conformed to the ethical guidelines of the Graduate School of Pharmaceutical Sciences, Osaka University.

4.3. Biochemical analysis

Serum alanine aminotransferase (ALT) and blood urea nitrogen (BUN) were measured using commercially available kits according to the manufacturer's protocols (WAKO Pure Chemical, Osaka, Japan).

4.4. Statistical analysis

Statistical analysis was performed by Student's *t*-test. $P < 0.05$ considered statistically significant.

Acknowledgements: The authors thank all members of our laboratory for their encouragements and useful comments. This study was partly supported by a grant from the Ministry of Health, Labor, and Welfare of Japan.

References

- Bartlett DW, Su H, Hildebrandt IJ, Weber WA, Davis ME (2007) Impact of tumor-specific targeting on the biodistribution and efficacy of siRNA nanoparticles measured by multimodality in vivo imaging. *Proc Natl Acad Sci USA* 104: 15549–15554.
- Burger KN, Staffhorst RW, de Vijlder HC, Velinova MJ, Bomans PH, Frederik PM, de Kruijff B (2002) Nanocapsules: lipid-coated aggregates of cisplatin with high cytotoxicity. *Nat Med* 8: 81–84.
- Caruthers SD, Wickline SA, Lanza GM (2007) Nanotechnological applications in medicine. *Curr Opin Biotechnol* 18: 26–30.
- Demoy M, Andreux JP, Weingarten C, Gouritin B, Guilloux V, Couvreur P (1999) In vitro evaluation of nanoparticles spleen capture. *Life Sci* 64: 1329–1337.
- Dutta D, Sundaram SK, Teeguarden JG, Riley BJ, Fifield LS, Jacobs JM, Addleman SR, Kaysen GA, Moudgil BM, Weber TJ (2007) Adsorbed proteins influence the biological activity and molecular targeting of nanomaterials. *Toxicol Sci* 100: 303–315.
- Fischer HC, Chan WC (2007) Nanotoxicity: the growing need for in vivo study. *Curr Opin Biotechnol* 18: 565–571.
- Hartmann JT, Kanz L, Bokemeyer C (1999) Diagnosis and treatment of patients with testicular germ cell cancer. *Drugs* 58: 257–281.
- Jansen RW, Molema G, Harms G, Kruijt JK, van Berkel TJ, Hardonk MJ, Meijer DK (1991) Formaldehyde treated albumin contains monomeric and polymeric forms that are differently cleared by endothelial and Kupffer cells of the liver: evidence for scavenger receptor heterogeneity. *Biochem Biophys Res Commun* 180: 23–32.
- Kamps JA, Morselt HW, Swart PJ, Meijer DK, Scherphof GL (1997) Massive targeting of liposomes, surface-modified with anionized albumins, to hepatic endothelial cells. *Proc Natl Acad Sci USA* 94: 11681–11685.
- Lu Y, Cederbaum AI (2006) Cisplatin-induced hepatotoxicity is enhanced by elevated expression of cytochrome P450 2E1. *Toxicol Sci* 89: 515–523.
- Medarova Z, Pham W, Farrar C, Petkova V, Moore A (2007) In vivo imaging of siRNA delivery and silencing in tumors. *Nat Med* 13: 372–377.
- Nel A, Xia T, Madler L, Li N (2006) Toxic potential of materials at the nanolevel. *Science* 311: 622–627.
- Nishimori H, Kondoh M, Isoda K, Tsunoda S, Tsutsumi Y, Yagi K (in press) Silica nanoparticles as hepatotoxicants. *Eur J Pharm Biopharm*.
- Oberdorster G, Oberdorster E and Oberdorster J (2005) Nanotoxicology: an emerging discipline evolving from studies of ultrafine particles. *Environ Health Perspect* 113: 823–839.
- Ozols RF, Young RC (1991) Chemotherapy of ovarian cancer. *Semin Oncol* 18: 222–232.
- Ramesh G, Zhang B, Uematsu S, Akira S, Reeves WB (2007) Endotoxin and cisplatin synergistically induce renal dysfunction and cytokine production in mice. *Am J Physiol Renal Physiol* 293: F325–F332.
- Vallet-Regi M, Balas F, Arcos D (2007) Mesoporous materials for drug delivery. *Angew Chem Int Ed Engl* 46: 7548–7558.
- Vandenbogaerde J, Schelstraete J, Colardyn F, Heyndrickx A (1984) Paraquat poisoning. *Forensic Sci Int* 26: 103–114.
- Witjes JA (1997) Current recommendations for the management of bladder cancer. *Drug therapy*. *Drugs* 53: 404–414.

